Hydrol. Earth Syst. Sci. Discuss., https://doi.org/10.5194/hess-2017-756
Manuscript under review for journal Hydrol. Earth Syst. Sci.
Discussion started: 17 January 2018

Hydrology and Earth System Sciences
Open Access
Discussions

Spatiotemporal Patterns and Trends of Precipitation and Their Correlations with Related Meteorological Factors by Two Sets of Reanalysis Data in China

Jinhui Jeanne Huang[(1)] , Nan Zhang[(2)], Gyewoon Choi[(2)], Edward Arthur McBean[(1,3)] and Qian Zhang[(1,4)]

(1) College of Environmental Science and Engineering/Sino-Canada R&D Centre on Water and Environmental Safety, Nankai University, Tianjin China.

(2) Civil and Environmental Engineering, Incheon National University，Incheon，Republic of Korea.

(3) School of Engineering, University of Guelph, N1G 2W1 Guelph, Ontario, Canada

(4) Corresponding Author.

Corresponding author: Qian Zhang

Sino-Canada R&D Centre on Water and Environmental Safety , College of Environmental Science and Engineering, Nankai University, Tianjin 300457, PR China;

Phone: (86)22-8535-8816; Fax: (86)22-8535-8816; E-mail: qianer0403@126.com

Abstract

This paper investigates the spatial-temporal characteristics of the changes in precipitation for China and the influence of other meteorological factors on precipitation. Two reanalysis datasets at monthly scale, namely, the GLDAS2 phase 2 forcing data 0.5×0.5 (1948 ~ 2008) and National Centers for

Environmental Prediction (NCEP) data were employed. The Mann-Kendall trend test identified the annual and seasonal changes in four meteorological factors for precipitation, air temperature, long wave radiation and surface pressure. Confidence levels of 95% were taken as thresholds to classify the significance of positive and negative trends. The trend analysis was conducted in three storm zones (I-Eastern Monsoon Region, II-Northern Inland Region and III-Qinghai-Tibetan Plateau Region) specified by Wang (2002). The findings indicate:

1) Air temperature, specific humidity and downward long wave radiation, have strong correlation with precipitation, especially for the eastern monsoon region of China; while surface pressure has very weak correlation with precipitation.
2) Latent heat shows very strong correlation with precipitation throughout China except for a small, extremely arid area in north China where large portions of the area are deserts.
3) The correlation between the volumetric soil moisture with precipitation and latent heat are controlled by precipitation with the characteristics of high annual precipitation and high correlations.
4) For precipitation, an increasing tendency in precipitation for the southeastern monsoon region and a decreasing tendency for the northeastern monsoon region (the drier region) were observed.
5) Strong increasing tendencies for air temperature and downward long wave radiation, were observed in the northeastern monsoon region and the western area of Qinghai-Tibetan Plateau.
6) Due to changes in precipitation and air temperature and downward long wave radiation, the scarcity of water resources in northeastern monsoon region and flooding problems in southeastern monsoon region may become more severe.
7) The study shows that agricultural development in China may require a shift between northern and western areas to adapt to the shift in precipitation patterns.

Keywords: Climate Change, Mann-Kendall Trend Analysis, Correlation, Precipitation, Meteorological Factors

1 Introduction

With economic development, global climate change has been become an important issue since it may have large, direct impacts on several aspects of the hydrologic cycle, in particular, bringing severe damages as a result more frequent drought and flooding events, creating more challenging conditions for managing and using water resources (Trenberth, 2010). Since precipitation is the primary source of renewable water resources, changes in precipitation patterns will have substantial influence on the welfare of human beings, as well as the entire ecosystems. IPCC (2014) indicates that the spatial patterns of projected changes in precipitation are not uniform; for example, model projections indicate that precipitation will increase by more than 1 mm/day in the southwest China, and declines will occur in northern, western, and southern parts of China (IPCC WG I, Section 6.2.2).

Significant changes in extreme rainfall events and more frequent rainfall events have been reported using the historical data over many areas in the world (e.g. Manton et al., 2001; Klein Tank and Konnen, 2003; Liu et al., 2005; Fujibe et al., 2005; Groisman et al., 2005; Massari et al., 2017) and in China (e.g. Gong and Wang, 2002; Gemmer, 2004; Ye et al., 2004; Li, 2011; Min, 2011; Zhu, 2011; Stephenson, 2014; Guo et al., 2017). For example, Gong and Wang (2002) have revealed significant negative precipitation trends for different regions of eastern China from 1954-1998 and subsequently, positive trends from 1977 – 1998; Gemmer (2004) also observed negative precipitation trends in spring and autumn in eastern China and positive trends in summer, and negative precipitation trends in the north and north-east of China. The increasing trends of precipitation are more significant in western China, particularly in the northwest (Ye et al., 2004). Most of above studies investigated the trends by the ground station data. Due to limited densities of ground stations, and their abrupt variations in space, the analysis and characterization of precipitation at regional scales requires reanalysis data to fill the spatial and temporal gaps. This study uses two sets of reanalysis data namely, the GLDAS2 phase 2 forcing data 0.5×0.5 (1948 ~ 2008) and National Centers for Environmental Prediction (NCEP) data 1.875×1.904 (1948 ~ 2013) to evaluate trends of precipitation levels in China.

Inquiry into precipitation changes under future climate has long been a research need. Statistical assessments of changes in precipitation and associated meteorological factors from the observational records have provided significant evidence in understanding the changing climate (Gokmen, 2016). At present, increased air temperatures have been widely regarded as the major factor causing climate change. Many studies have shown that temperature and precipitation have positive correlations (Trenberth and Shea, 2005; Wu, 2012; and Zhang, 2013). However, some researchers have also observed both positive and negative trends in different locations (Trenberth and Shea, 2005, Mourre et al., 2016). For example, Trenberth and Shea (2005) showed that precipitation has reduced downward shortwave radiation reaching the earth's surface, resulting in surface cooling which may contribute to a negative correlation between precipitation and temperature.

In addition to temperature, some other meteorological and hydrological parameters may also have substantial influences on changes in precipitation (Liu, 2009; Gong, 2006). Gong (2006) stated that relative humidity was the most sensitive variable, in general, for the Yangtze River basin in China, followed by shortwave radiation, air temperature and wind speed. Liu (2009) analyzed climate change in Xinjiang Uygur Autonomous Region by investigating the relationship between annual precipitation with mean temperature, wind speed, low cloud cover, total cloud cover, specific humidity, pan evaporation, and diurnal temperature range. Lin reported that evapotranspiration is a key process in the hydrologic cycle and has significant influence on precipitation. Comprehensive analyses of the precipitation and its correlation with other meteorological factors are crucial to improving prediction of changing climates (Fang et al., 2014).

As stated above, the present research used two sets of reanalysis data to investigate the correlation between precipitation and other meteorological and hydrological factors including downward long-wave radiation, downward shortwave radiation, air temperature, specific humidity, surface pressure, wind speed, evapotranspiration, soil moisture, etc. Through correlation analysis, this study presents relationships between precipitation and many other meteorological and hydrological factors. The trends in precipitation and these meteorological and hydrological factors are also assessed in this study, including the trend analysis in seasonal and annual scales. China has very rich varieties of topographic and climatic characteristics. The association of the correlation analysis and trend analysis with topographic and climatic characteristics are also assessed in this study. Two procedures are utilized herein to perform the correlation analysis and trend analysis as described below.

2 Materials and Methods

2.1 Data

In this study, two reanalysis datasets were used, namely, the Global Land Data Assimilation System (hereafter, GLDAS) and a reanalysis dataset from National Centers for Environmental Prediction (hereafter, NCEP). For atmospheric forcing datasets, the common datasets are as follows: (1) NCEP's Global Data Assimilation System (GLDAS); (2) NASA's Goddard EOS Data Assimilation System (GEOS); (3) The European Center for Medium Range Weather Forecasting (ECMWF); (4) The Princeton Global Meteorological Forcing Dataset; (5) Naval Research Laboratory Precipitation; (6) NASA/GSFC TRMM 3B42RT Real-time Huffman Precipitation; (7) PERSIANN Precipitation; (8) Disaggregated CMAP Precipitation; (9) Air Force Weather Agency (AFWA) Radiation; (10) NOAA/CPC CMORPH Precipitation; (11) NASA/GSFC TRMM 3B42(V6) Precipitation. (http://ldas.gsfc.nasa.gov/). GLDAS uses the following atmospheric metrics: 1979-1993, bias-corrected ECMWF Reanalysis data (Berg et al., 2003); 1994-1999, bias-corrected NCAR Reanalysis data (Berg et al., 2003); 2000, NOAA/GDAS atmospheric analysis fields; 2001-2007: a combination of NOAA/GDAS atmospheric analysis fields, spatially and temporally disaggregated NOAA Climate Prediction Center Merged Analysis of Precipitation (CMAP) fields, and observation-based downward shortwave and longwave radiation fields derived using the method of the Air Force Weather Agency's AGRicultural METeorological modeling system (AGRMET).

Global Land Data Assimilation System Version 2 (GLDAS2) dataset is bias-corrected reanalysis data, from the Terrestrial Hydrology Research Group, Princeton University. It can be downloaded at its homepage (http://hydrology.princeton.edu/). The GLDAS2 data have been generated using upgraded versions of Land Surface Models (LSMs). Compared with GLDAS1, GLDAS3 has been enhanced by using the global meteorological forcing data set from Princeton University. It was produced by merging satellite and ground-based observational data products using advanced LSMs and data assimilation techniques. Its temporal coverage has been extended back to 1948.

GLDAS2 is a series of land surface forcing data, such as precipitation, surface meteorology and radiation; state data such as soil moisture, temperature and snow; and flux data such as evaporation and sensible heat flux data which were simulated by LSM. In this research, data between 1948 and 2008 were used with resolution of 0.5x0.5, and the meteorological factors in monthly scale are precipitation, air temperature, specific humidity, downward longwave radiation, surface pressure, and wind speed.

The NCEP/NCAR is one kind of Physical Sciences Division (PSD) Gridded Climate Datasets. PSD maintains a collection of reanalysis datasets for use in climate diagnostics and attribution. NCEP/NCAR Reanalysis data set (1948 - present), and it was the first of its kind of National Oceanic and Atmospheric Administration (NOAA). It has been continually updated, gridded daily and monthly data set that represents the state of the Earth's atmosphere, incorporating observations and numerical weather prediction (NWP) model. NCEP used the same climate model that was initialized with a wide variety of weather observations: ships, planes, RAOBS, station data, satellite observations and many more. It was a joint product from the National Centers for Environmental Prediction (NCEP) and the National Center for Atmospheric Research (NCAR). The NCEP/NCAR reanalysis mainly concentrates on using initialization at a smaller scale atmospheric mode, and climate assessment. NCEP also includes Climate Forecast System Reanalysis (CFSR). NCEP not only has been among the most used NCEP products in history, but continued use in the future is expected with a more modern data assimilation system and forecast model (Suranjana Saha, 2010). This study focused on the analysis of climate variability for a set of surface variables including the monthly mean precipitation, 2m surface air temperature, surface pressure, latent heat, soil moisture, upward solar radiation, downward longwave radiation**,** momentum flux, sensible heat, and surface roughness. These data were downloaded from the National Oceanic and

Atmospheric Administration-Earth System Research Laboratory (NOAA-ESRL) (http://www.esrl.noaa.gov/). The temporal coverage is from 1948/01 to present, and spatial coverage is T62 Gaussian grid (192×94), the latitude is 88.542N ~ 88.542S, and longitude is 0E ~ 358.125E. Basic information for the two datasets is shown on Table 1.

2.2 Methodology

2.2.1 Correlation Analysis

In the theory of probability and statistics, Student's t-distribution (called t-distribution) was applied to evaluate the mean of a symmetrically distributed population where the sample size is small and population standard deviation is unknown.

The first dataset was from 1948 to 2008, totaling 61 years data, so the population n = 61yrs×12 mons= 732 mons. Based on the one-sided t-distribution table, when df=730 (degree of freedom, n-2=730), for the 99% confidence level, t* = 2.326.

$$t^* = r\frac{\sqrt{n-2}}{\sqrt{1-r^2}} \tag{1}$$

Following the Equation (1), r = ±0.086

Through the Pearson product – moment correlation coefficient (Pearson's r), two variables x and y can be measured by the linear correlation, giving a value between +1 and -1. The formula was

$$r = \frac{\sum(x_i-\acute{x})(y_i-\acute{y})}{\sqrt{\sum(x_i-\acute{x})^2\sum(y_i-\acute{y})^2}} \tag{2}$$

Based on the coefficient, r, if the value of r exceeds 0.086, it has 99% confidence level that the correlation is significant.

2.2.2 Mann-Kendall Test

The Mann-Kendall Test (1938) has also been widely used in the meteorological field. Through use of the Mann-Kendall Test, the trends of the meteorological factors, e.g. precipitation and air temperature can be assessed. The Mann-Kendall test can evaluate the change tendency with long-term time series for predicting the influence of potential climate change. In the past, many parametric and nonparametric methods have been used for trend detection(Shi et al., 2015). Nonparametric methods usually require less burdensome calculations because they are generally not related specifically to the parameters of a given distribution and do not require any assumptions other than independence. The Mann-Kendall trend test is a rank-based non-parametric approach that tests the randomness against trends in time series datasets. It can be used to detect trends that are monotonic but not necessarily linear. The rank tests are highly useful for the investigators since these tests are completed relatively quickly with an efficiency of approximately 95% relative to the t-test for large size and even higher for small samples (Huang et al., 2016). The Mann-Kendall trend test compares each value of time-series data with the remaining values in sequential order, accounting for the number of times of increasing or decreasing. It does not require the assumption of normality and only indicates the direction but not the magnitude of significant trends. The Mann–Kendall trend test has a broad range of applications in hydrologic and climate-related trend analysis (e.g. Tong et al., 2007, Huo et al., 2008, McBean and Motiee, 2008, Kustu et al., 2010).

The null hypothesis (H_0) in the Mann-Kendall test is that the data (x_1, x_2, x_3,...x_n) are independent and randomly ordered. The alternative hypothesis H_1 of a two-sided test is that the distributions of x_k and x_j are not identical for all k, j.

The confidence level of 95% was taken as thresholds to classify the significance of positive and negative meteorological factor trends. The trend is considered to be statistically significant if it is

Hydrol. Earth Syst. Sci. Discuss., https://doi.org/10.5194/hess-2017-756
Manuscript under review for journal Hydrol. Earth Syst. Sci.
Discussion started: 17 January 2018

significant at the 5% level (P < 0.05). The computational procedure for the Mann–Kendall test is described as follows:

1) The entire data set consists of n data points. N_k and N_j are two sub-sets of data where the time-series x_k is from $i = 1, 2, . . . ,n - 1$, and x_j from $j = i + 1 , . . ., n$

2) Each data point x_i is used as a reference point and is compared with all the x_j data points such that:

$$\mathrm{sign}(\theta) = \begin{cases} 1, & \theta > 0 \\ 0, & \theta = 0 \\ -1, & \theta < 0 \end{cases} \quad (3)$$

where $\theta = \mathrm{s}ign(k_k - x_j)$.

3) The Kendall's S-statistics is estimated by

$$S = \sum_i^{n-1} \sum_{k=i+1}^{n} sign(x_k - x_j) \quad (4)$$

4) The variance for the S-statistics is determined by:

$$Var(S) = \frac{1}{18}\left[n(n-1)(2n+5) - \sum_{p=1}^{g} t_p(t_p - 1)(2t_p + 5)\right] \quad (5)$$

where g is the number of tied groups (a tied group is a set of sample data having the same value), and t_p is the number of data points in the p^{th} group. For example, for a data set of {2, 3, 5, 3, 5, 3}, it has n = 6, g = 2, t_1 = 2 for the tied value 5, while t_2 = 3 for the tied value 3.

5) The parameter Z_c is given as

$$Z_c = \begin{cases} \frac{S-1}{\sqrt{Var(S)}}, & S > 0 \\ 0, & S = 0 \\ \frac{S+1}{\sqrt{Var(S)}}, & S < 0 \end{cases} \quad (6)$$

where Z_c is the test statistic and follows a standard normal distribution.

The test statistic Z_c is used as a measure to identify the significance of the trend. In fact, this test statistic is used to test the null hypothesis, H_0, which means no monotonic trend in the data. If $|Z_c|$ is greater than $>Z_{\alpha/2}$, where α represents the chosen significance level (usually α = 5% with $Z_{1-\alpha/2}$=1.96), the null hypothesis is rejected, meaning that the trend is significant with the confidence level at the magnitude of 1- α /2 (97.5%).

The Mann-Kendall statistic S was calculated as Equation (4), the variance for the statistic S was defined by formula (5), and the test statistic Z was estimated from formula (6). A significant level is determined when |Z| > Z. In this case, the trend is considered as significant at the confidence level determined by Z (e.g. 95% when $Z_{1-\alpha/2}$=1.96).

The Mann-Kendall test method was adopted to investigate the possible trends in monthly data series for precipitation, air temperature, downward long wave radiation, specific humidity, and surface pressure, sensible heat, latent heat and volumetric soil moisture.

2.2.3 Storm Zones

Wang (2002) divided China into three storm zones based on the topographic features and the two precipitation extreme indicators, namely, H24m (which is the 24 hour annual maximum precipitation) and T50 (which is the annual average of days that daily rainfall was larger or equal to 50mm). The three main boundary lines are:

(1) Zone I: Southeastern side of the line along Qinling Mountains – Taihang Mountains – Xiao Hinggan Mountains where H24 = 70mm and T50 = 1day.

(2) Zone II: Northern margin of the line along Qinghai – Tibetan Plateau where H24m < 50mm. The area is called the Northern Zone below.

(3) Zone III: Western side of the line along Qinghai – Tibetan Plateau where H24m < 70mm and T50 < 1day. It is referred to as the Western Zone below.

These zones are also referred to as, respectively, Southeast, Northern and Western China herein. The areas are shown in Figure 1 as separated by yellow lines. Zone I occupies about 45% of China and has half of its area along the east coast line of China. It is also called the eastern monsoon region. This region is strongly influenced by the monsoon climate and has the highest average annual precipitation amongst the three zones. The major storm zones are also located in this region. The north portion of Zone I has lower frequencies of storms than the south portion; however, the most extreme storms in China occur in the northern portion of Zone I (Wang 2002). Zones II and III are all inland areas. Arid and semi-arid climate are the dominant climates for Zone II. Zone II is also called Northwestern arid and semi-arid region, which occupies 35% of China. Most of Zone III area is located in Qinghai-Tibetan Plateau. Qinghai- Tibetan Plateau is the highest Plateau in the world and the largest Plateau in China occupies an area of 2.3 million km^2, and has an average altitude exceeding 4000 m. Due to its extreme, high altitude and cold climate, storms rarely occur in this region and have lower precipitation than the other two regions. Zones I, II and III each have very unique topographic and climatic characteristics. In this study, the correlation between precipitation and other meteorological factors as well as the trends of meteorological factors were evaluated and analyzed based on the characteristics of the three zones.

3 Results and Discussions

3.1 Correlation Results

To assess the influence of various meteorological factors on precipitation, correlation analysis was conducted for China. Figure 2 shows the correlation results of precipitation with air temperature, downward long wave radiation, and surface pressure of the two datasets: GLDAS2 forcing data and NCEP data. A comparison of the results from the two datasets was also performed. Figure 3 shows the correlation results of precipitation with specific humidity of GLDAS2 and with volumetric soil

Hydrol. Earth Syst. Sci. Discuss., https://doi.org/10.5194/hess-2017-756
Manuscript under review for journal Hydrol. Earth Syst. Sci.
Discussion started: 17 January 2018

moisture, latent heat flux and sensible heat net flux. The color bar shows that the correlations between precipitation and all other meteorological factors exceed 0.09, which indicates that the correlations are significant at confidence level above 99%.

Air temperature has long been considered to have strong influence on precipitation. Warmer temperatures may accelerate the global circulation and make the precipitation extremes occur more frequently. The GLDAS2 forcing data and NCEP data both show that the precipitation and air temperature have strong correlation in Zone I (except a small portion of the eastern area) and Zone III (except the western area); while GLDAS2 shows stronger correlation than NCEP in Zone II; alternatively, NCEP shows stronger correlation than GLDAS2 in the western area of Zone III and a small portion of the eastern area.

The downward long wave radiation is an important meteorological factor which represents the energy from atmosphere. It is related to the temperature and water vapor distribution in the atmosphere. For downward long wave radiation, in a very similar fashion as the correlation between precipitation and air temperature, both the GLDAS2 data and NCEP data show strong correlation in Zone I (except a small portion of the eastern area) and Zone III (except the western area). GLDAS2 shows stronger correlation than NCEP in Zone II; alternatively, NCEP shows stronger correlation than GLDAS2 in the western area of Zone III and a small portion of the eastern area. It is observed that there are large discrepancies between the results from GLDAS2 and the results from NCEP. However, the results for downward long wave radiation and air temperature related with precipitation, show almost identical spatial patterns by GLDAS2 as well as by NCEP. This may indicate a strong correlation between temperature and downward long wave radiation.

For surface pressure, the results from both GLDAS2 and NCEP show very good agreement. Both show that the surface pressure has very weak correlation with precipitation than air temperature and downward long wave radiation for most areas in China; alternatively, in the western portion of Zone III, the correlation is stronger than other areas. It may due to very high latitudes of the western portion of Zone III.

Figure 3 shows the relationship of precipitation with other meteorological factors including specific humidity from GLDAS2, and latent heat, sensible heat, volumetric soil moisture from NCEP. Specific humidity is a very useful factor in meteorology when studying the spatial-temporal patterns of precipitation as it represents the ratio of the mass of water vapor in air to the total mass of the mixture of air and water vapor. For the correlation between precipitation and specific humidity, it shows almost the same spatial pattern as the air temperature and the downward long wave radiation.

For the correlation of volumetric soil moisture related with precipitation, the southern half of China shows strong correlation, while the northern half of China shows very weak correlation.

For the land surface energy balance, the net radiation (NR) is equal to latent heat flux (LE) plus sensible heat flux(H) plus ground heat flux(G) (Eq. 7), which governs the hydrological, biogeochemical, and ecological process at the Earth's surface (Liang et al., 2014):

$$NR=LE+H+G \tag{7}$$

The energy balance of land surface is the driving force for precipitation and has large influence on precipitation in both global and local schemes. Due to the latent heat flux being the key component to connect the energy cycle and hydrological cycle, the latent heat flux is one of the focus of this study, the correlation between latent heat and other meteorological factors including precipitation, air temperature and soil moistures were analyzed. The results are shown in Figures 3 and 4.

For the correlation of latent heat related with precipitation, most areas of China show a strong relationship except a very small portion in the north of Zone II, which is an extremely arid area with large portions occupied by deserts. For the correlation of sensible heat net flux, it shows a very similar spatial pattern of the correlation between surface pressure and precipitation.

The correlations between latent heat and air temperature (NCEP) are shown in Figure 4. Zone I (East monsoon region) and Zone III (Qinghai- Tibetan Plateau) show very strong correlations as well as in the southern portion of Zone II (the arid and semi-arid area); alternatively, most areas of Zone II (mostly in the arid area) show a much weaker correlation (or non-significant correlation) between air temperature and latent heat. This finding supports the ideas of Brutsaert (1998) regarding the paradox of decreasing evaporation and evapotranspiration under increasing temperature conditions in arid and

Hydrol. Earth Syst. Sci. Discuss., https://doi.org/10.5194/hess-2017-756
Manuscript under review for journal Hydrol. Earth Syst. Sci.
Discussion started: 17 January 2018

semi-arid regions. Regarding the correlations between latent heat and soil moisture (NCEP), there is a very strong correction in the southern portion of Zone I (eastern monsoon region) with high annual precipitation, while the northern portion of Zone I with less annual precipitation and Zones II and III show much weaker/no significant correlations. This may imply that with the latent heat dependency on soil moisture when the water supply (precipitation) is sufficient, with much less water (lower precipitation), the amount of latent heat would be highly influenced by other meteorological factors.

3.2 Mann-Kendall Analysis

From knowledge of the correlation between the precipitation and all other meteorological factors, the trend analysis for precipitation and all other meteorological factors were conducted using the Mann-Kendall method.

In order to study the spatial – temporal pattern in China, seasonal patterns of factors are important. Trend analysis for all the meteorological factors were completed for each season, as well as in the annual scale. Spring refers to March, April and May; Summer refers to June, July and August; Fall refers to September, October and November and Winter refers December, January and February. The trends identified by Mann-Kendall method are illustrated in Figures 5 through 9.

From the color bar, the dark burgundy color indicates the Z value is larger than 2, meaning that the trend of increase is significant at a confidence level exceeding 95%; alternative, the dark blue color indicates the Z value is less than -2, meaning that the trend of decrease is significant at a confidence level exceeding 95%.

3.2.1 Trends in Precipitation

Results from GLDAS2 dataset: As shown in Figure 5, the southern portion of Zone I (eastern monsoon region) show strong decreasing trends in spring and fall seasons, increasing trends in summer, a slightly increasing trend (with half of the above-indicated area) in winter and annual scale, while a slightly decreasing trend (with another half of the above-indicated area) in winter and annual scale.

However, there are decreasing trends in spring and fall. The northern portion of Zone I (the drier region of Zone I) shows decreasing trends on the annual scale and all seasons except in spring. For Zone II, the western portion of Zone II shows strong increasing trends in all seasons and at the annual scale, while the eastern portion of Zone II shows strong decreasing trends in all seasons and at the annual scale. Zone III shows very consistent strong increasing trends in all seasons and in annual scale for the entire area. The source waters for both Yangtze River and Yellow River are all located in Zone III.

Results from NCEP dataset: As shown in Figure 5, only a small portion in the southern end of Zone I shows strong increasing trends in the seasons of spring and winter and in the annual scale, while most the other areas of Zone I show strong decreasing trends in these seasons and in the annual scale, while in the fall, most the areas in Zone I show a strong decreasing trend and in summer, more than half of the area in Zone I along the coast area shows a strong increasing trend in summer. For Zone II, the results show a consistent decreasing trend for the entire area in all the seasons and in the annual scale. A small portion of area in the middle of Zone III shows increasing trends in all seasons and at the annual scale, while all the other areas in Zone III show an opposite trend (decreasing).

Comparing the results by the two datasets (GLDAS2 and NCEP), it was observed that the two datasets agree in terms of trends for Zone I in all seasons and annual scales, except the northern portion of Zone I in the spring. They all indicated an increasing tendency for the monsoon region and a decreasing tendency for the northern portion (the drier region). The northern portion of Zone I is highly industrialized and with intensified agriculture development. The decreasing trend of precipitation in the annual scale will intensify the scarcity of water resources in this region. The increasing trends in summer for the monsoon region may also increase the risk of flooding during the flood season. Results for both datasets agree for the eastern portion of Zone II, showing opposite tendencies for the western areas in all seasons and at the annual scale. For most areas of Zone III except the small potion in the middle, opposite tendencies are evident.

Hydrol. Earth Syst. Sci. Discuss., https://doi.org/10.5194/hess-2017-756
Manuscript under review for journal Hydrol. Earth Syst. Sci.
Discussion started: 17 January 2018

3.2.2 Trends in Other Meteorological Factors

Results for Meteorological Factors: Air Temperature, Downward Long Wave Radiation, Surface Pressure, Specific Humidity, Sensible Heat Net Flux, and Latent Heat Net Flux

The three meteorological factors (air temperature, downward long wave radiation, surface pressure) are both available in the two datasets: GLDAS2 and NCEP, so the trends of these three factors were analyzed and compared in this study.

Air Temperature: The left column of Figure 6 shows the tendency of air temperature from GLADAS2 dataset in all the seasons and at the annual scale. As shown in Figure 6, the entire Zone I shows a strong increasing trend by the burgundy color (indicating Z>2.0) for the annual scale, only small portions in southwestern part of Zone I show no trend (with Z < 0.5). All the seasons function similarly to the annual scale except the summer season. In summer, only the northern areas of Zone I show a strong increasing trend while the southern area of Zone I show a strong decreasing tendency. For Zone II, the entire zone shows a strong increasing in all seasons and at the annual scale, except for the summer season. In summer, a small area in the west and a small area in the southeastern region show a strong decreasing trend, while the remainder of the area shows a strong increasing trend. For Zone III, most of the area shows a strong increasing tendency while only a small area in the eastern part does not show trends with significant level of confidence above 95%.

The right column of Figure 6 shows the tendency of air temperature in all the seasons and in the annual scale from NCEP. For Zone I, for the annual scale, the northern portion shows strong increasing trends while the southern portion shows a strong decreasing tendency and both with significant level exceed 95%. Winter and spring show similar trends as the annual scale, while in the summer, there are more areas showing increasing tendency and only a small portion in southern area shows strong decreasing tendency. In the fall, only about one-third of Zone I in the middle shows a strong increasing tendency, with the remaining areas showing neither significant trends nor strong decreasing trends. For Zone II, the spatial patterns for annual and seasonal scales make a good agreement. Most areas of Zone II show decreasing tendencies or no trend in the annual and seasonal scales, only a small portion of

Zone II along the boundary with Zone I shows strong increasing trends. For Zone III, the spatial patterns for the annual scale and all seasonal scales except fall indicate good agreement. The western portion of Zone III shows strong increase tendency while the remainder of the area shows decreasing tendency. For the fall season, the area with increasing tendency has decreased to a small 'dot' in the far west, while other areas show no significant tendency or strong decreasing tendency.

To compare the results from the two datasets, it was observed that they agree in the northern portion of Zone I (the lower annual precipitation area of the east monsoon region), the area of Zone II along the boundary with Zone I in the northern and western areas of Zone III. The trends in the two datasets in air temperature for all the other areas show the opposite directions of trends.

Downward long wave radiation: The trends of downward long wave radiation for entire China in all the seasons and in the annual scale are indicated in Figure 7.

The column on the left of Figure 7 displays the tendency of downward long wave radiation from GLDAS2 dataset. Only small portions of Zone I along the southeast coast shows decreasing trends in all seasons and in the annual scales while all the other areas show strong increasing trends, which means that these areas are receiving more energy with time. Additionally, in the summer season, the areas with decreasing trends are larger than other seasons as well as are larger than in the annual scale. For Zone II (the arid and semi-arid region), essentially the entire area shows increasing trends for the annual scale, fall and winter seasons, only a small portion of Zone II, located in the middle west show a strong decreasing trend; in spring, a small portion of the area, located in the central west of Zone II with an area about 1/4 of Zone II, shows a strong decreasing trend, while the other areas shows the same extent of increasing trends as showing in annual scale and all other seasons; summer is the only season with almost the entire area of Zone II showing increasing trends. For Zone III, almost the entire area shows decreasing trends in spring, winter and in the annual scale, while in the summer and fall, about half of the area shows decreasing trends while the other half shows increasing trends with different spatial patterns in the two seasons.

The right column of Figure 7 displays the tendency of downward long wave radiation from NCEP. For Zone I, the entire area show strong decreasing trends observed in all seasons and in the annual scale; except in summer, the southern half of Zone I shows a strong increasing trend. For Zone II, the strong decreasing trends are shown in all seasons and the annual case. For Zone II, the entire zone shows a strong decreasing trend in all seasons and the annual scale. For Zone III, spring and winter seasons and annual case show decreasing trend with the exception of the central part of the western area, while a small portion of Zone III shows a strong increasing trend. The fall season shows the stronger decreasing trends relative to other seasons and the annual scale.

Surface pressure: The left column of Figure 8 indicates the surface pressure trends from GLDAS2 datasets, throughout Zones I, II, and III, the increasing tendencies are shown in all seasons and in the annual scale. The right column of Figure 8 shows surface pressure trends from NCEP reanalysis data. It is observed that Zones I, II, and III present the increasing tendency in all seasons and in the annual scale. Both of the datasets show the same increasing trend results.

Specific humidity, land evapotranspiration also play important roles in the hydrologic field. This study analyzed specific humidity, sensible heat and latent heat to estimate the evaporation. Figure 6 shows specific humidity, sensible heat net flux and latent heat net flux trends assessed using the Mann-Kendall method.

Specific humidity is a ratio of the water vapor mass to the air parcel's total mass. Humidity itself is a climate variable, affected by rainfall and air temperature, and plays an important role in weather forecasts. As shown in the first vertical column of Figure 6 (derived from GLDAS2 dataset), for Zone I, the southern areas show increasing tendencies in spring and the annual scale, while a decreasing trend was observed in summer, fall and winter seasons; for Zone II, spring obviously shows a decreasing trend through whole areas, other seasons and the annual scale show decreasing trends in most areas, while small western areas show increasing trend; for Zone III, whole areas show decreasing trend in all seasons and the annual scale.

Sensible heat net flux: is heat exchanged by a body or thermodynamic system that changes the temperature, and some macroscopic variables of the body, but leaves unchanged certain other macroscopic variables, such as volume or pressure; this is in contrast to latent heat. As shown in the

Hydrol. Earth Syst. Sci. Discuss., https://doi.org/10.5194/hess-2017-756
Manuscript under review for journal Hydrol. Earth Syst. Sci.
Discussion started: 17 January 2018

Hydrology and Earth System Sciences
Discussions

middle column of Figure 6 (derived from NCEP dataset), most areas in China show strong increase trends except in the fall season. In the fall, small portions of Zone I, II and III show decreasing trends.

Latent heat net flux: Latent heat represents the energy released or absorbed by a body or a thermodynamic system during a constant-temperature process. As shown in the right column of Figure 6 (derived from NCEP dataset), latent heat flux for almost all areas in China show decreasing trends except half the area of Zone I in the west showing increasing trends.

3.3 The Impacts on Agriculture Practices

Climate change, water shortages and food security are global concerns to human society. Figure 10 presents the land use map with the rainfall zoning of China in seven classifications: urban impervious area, forest, water, cropland, pasture, barren and others. The resolution of the land use map is in 250m and it is obtained from the State of Earth System Science Data Platform (http://westdc.westgis.ac.cn/).

From the view of the proportion of cropland in the three rainfall zones, Zone I covers large and intensified cropland. The water demand for irrigation accounts for substantial portions of the total water need in this area. These two datasets showed precipitation decreasing trends in this cropland area which means that these areas will face problems of water shortage. The same situation occurs for the Yellow Basin at rainfall, for Zone II with intensified cropland, the precipitation trend is also decreasing. Therefore, alternative cropping patterns with high-yield/less-water-demand crops may need to be employed to adapt to the climate change. On the other hand, precipitation in western areas shows increasing trends. The croplands are relatively smaller than other areas. It is beneficial for the agricultural development in this area.

4 Conclusions

This study investigated the correlations between precipitation and other meteorological parameters; the spatial and temporal pattern for precipitation and some meteorological parameters with high correlate with precipitation identified over China. The GLDAS2 forcing data and NCEP data were used and compared. The specific findings as shown below:

4.1 Correlation Analysis

The correlation analysis indicated:

1) The two data sets both show that the two meteorological parameters: air temperature and downward long wave radiation have strong correlation with precipitation, especially for the eastern monsoon region of China; while surface pressure has very weak correlations with precipitation .
2) By GLDAS2 data set, the specific humidity shows almost the same spatial pattern as the air temperature and downward long wave radiation, with strong correlation with precipitation.
3) By NCEP data:
   a) The volumetric soil moisture only shows strong correlation with precipitation in southern China where the rainfall is more frequent and shows very weak correlation in northern China where the rainfall is much less than southern China.
   b) The latent heat shows very strong correlation with precipitation for China except for a small, extremely arid area in north China with large portions of the area occupied by deserts.
   c) The latent heat also shows strong correlation with air temperature except for extremely arid area in north China.
   d) The correlation between latent heat and soil moisture was observed that it was controlled by annual precipitation
4) The results show that in China, the agriculture development may need to shift from north area and western area to adapt to the shift of precipitation patterns.

These results indicate that air temperature, downward long wave radiation, specific humidity, soil moisture, latent heat, and sensible heat are correlated with precipitation, and hence impact the hydrologic cycle. The significant correlations: between latent heat and temperature, latent heat and soil moisture, were found that land and atmosphere interactions may influence the water cycle, which would be interesting to do further investigation.

4.2 Trend Analysis

The Mann-Kendall trend analysis showed:

1) For precipitation, both the GLDAS2 and NCEP data sets indicate an increasing tendency for the southern monsoon region and a decreasing tendency for the northern monsoon region (the drier region).
2) For air temperature and downward long wave radiation, the data indicate the north portion of the monsoon region and the western area of Qinghai-Tibetan Plateau with strong increasing tendency.
3) For surface pressure, the increasing trend was observed with different temporal scales by two datasets.
4) For specific humidity, the trend derived from GLDAS2 shows a decreasing tendency in most parts of China in all the temporal scales except for the southern area of Monsoon region in spring and the annual scale.
5) For sensible heat net flux, the trend derived from NCEP shows an increasing tendency in most parts of China in all the temporal scales except the fall season.
6) For the latent heat net flux, the trend derived from NCEP shows a decreasing tendency in most parts of China in all the temporal scales except most the areas of Qinghai-Tibetan Plateau.

Because the northern area of Monsoon region in China is highly industrialized and with intensified agriculture development, the decreasing trend of precipitation may lead to scarcity of water resources in this region, resulting in more severe economic development in this area. The increasing air temperatures and downward long-wave radiation may indirectly encourage the agriculture development in this region, which may have huge influences on water demand. These are all the factors which need to be considered in a broader range of water resources management.

Acknowledgements:

This research was financially supported by National Natural Science Foundation of China (41561124015) and Ministry of Science and Technology (2016YFC0400709).

Hydrol. Earth Syst. Sci. Discuss., https://doi.org/10.5194/hess-2017-756
Manuscript under review for journal Hydrol. Earth Syst. Sci.
Discussion started: 17 January 2018

References

Brutsaert, W. and Parlange M. B.: Hydrologic cycle explains the evaporation paradox, Nature, 396, 30, 1998.

Fang G H, Yang J, Chen Y N, et al. Comparing bias correction methods in downscaling meteorological variables for a hydrologic impact study in an arid area in China[J]. Hydrology & Earth System Sciences Discussions, 2014, 11(11):2547-2559.

Fujibe F, Yamazaki N, Katsuyama M, et al.: The increasing trend of intense precipitation in Japan based on four-hourly data for a hundred years, Sola, 1, 41-44, 2005.

Gemmer M, Becker S, Jiang T.: Observed monthly precipitation trends in China 1951–2002, Theoretical and applied climatology, 77, 39-45, 2004.

Gokmen M. Spatio-temporal trends in the hydroclimate of Turkey for the last decades based on two reanalysis datasets[J]. Hydrology & Earth System Sciences Discussions, 2016, 20(9):1-16.

Gong D Y, Ho C H. Shift in the summer rainfall over the Yangtze River valley in the late 1970s[J]. Geophysical Research Letters, 2002, 29(10): 78-1-78-4.

Groisman P Y, Knight R W, Easterling D R, et al. Trends in intense precipitation in the climate record, Journal of climate, 18, 1326-1350, 2005.

Guo R, Liu Y, Zhou H, et al. Precipitation downscaling using a probability-matching approach and geostationary infrared data: An evaluation over six climate regions[J]. Hydrology & Earth System Sciences Discussions, 2017:1-26.

Huang J J, Li Y, Yin J, et al. Precipitation regional extreme mapping as a tool for ungauged areas and the assessment of climate changes[J]. Hydrological Processes, 2016, 30(12):1940-1954.

Huo, Z., Feng, S., Kang, S., Li, W., and Chen, H.: Effect of climate changes and water-related human activities on annual stream flows of the Shiyang river basin in arid north-west China. Hydrological Processes, 22, 3155-3167, 2008.

IPCC: Fifth assessment report climate change 2014, Paris, http://www.ipcc.ch/, 2014.

Klein Tank A M G, Können G P.: Trends in indices of daily temperature and precipitation extremes in Europe, 1946-1999, Journal of Climate, 16, 3665-3680, 2003.

Li Z, He Y, Wang C, et al.: Spatial and temporal trends of temperature and precipitation during 1960–2008 at the Hengduan Mountains, China, Quaternary International, 236, 127-142, 2011.

Liu B, Feng J M, Ma Z G, et al.: Characteristics of climate changes in Xinjiang from 1960 to 2005, Clim Environ Res, 14, 414-426, 2009.

Liu B, Xu M, Henderson M, et al.: Observed trends of precipitation amount, frequency, and intensity in China, 1960–2000, Journal of Geophysical Research: Atmospheres (1984–2012), 110, 2005.

Manton M J, Della‐Marta P M, Haylock M R, et al.: Trends in extreme daily rainfall and temperature in Southeast Asia and the South Pacific: 1961–1998, International Journal of Climatology, 21, 269-284, 2001.

Massari C, Crow W, Brocca L. An assessment of the accuracy of global rainfall estimates without ground-based observations[J]. Hydrology & Earth System Sciences Discussions, 2017:1-24.

McBean E, Motiee H. Assessment of impact of climate change on water resources: a long term analysis of the Great Lakes of North America [J]. Hydrology and Earth System Sciences, 2008, 12(1): 239-255.

McBean E. A. and Rovers, F. A.: Chapter 11, Nonparametric procedure, in statistical procedures for analysis of environmental monitoring data and risk assessment, Prentice Hall PTR, New Jersey, ISBN 0-13-675018-4, 1998.

Min S K, Zhang X, Zwiers F W, et al.: Human contribution to more-intense precipitation extremes, Nature, 470, 378-381, 2011.

Mourre L, Condom T, Junquas C, et al. Spatio-temporal assessment of WRF, TRMM and in situ precipitation data in a tropical mountain environment (Cordillera Blanca, Peru)[J]. Hydrology & Earth System Sciences Discussions, 2016, 12(7):6635-6681.

Shi P, Wu M, Qu S, et al. Spatial Distribution and Temporal Trends in Precipitation Concentration Indices for the Southwest China[J]. Water Resources Management, 2015, 29(11):3941-3955.

Stephenson T S, Vincent L A, Allen T, et al.: Changes in extreme temperature and precipitation in the Caribbean region, 1961–2010, International Journal of Climatology, 2014.

Tong, L., Kang, S., and Zhang, L.: Temporal and spatial variations of evapotranspiration for spring wheat in the Shiyang river basin in northwest China. Agricultural Water Management. 87(3), 241-250, 2007.

Trenberth K E, Shea D J. Relationships between precipitation and surface temperature[J]. Geophysical Research Letters, 2005, 32(14).

Trenberth K E.: Changes in precipitation with climate change, Climate Research, 47, 123, 2011.

Wang, J. Q.: Chapter 12, The Rainfall Zoning, in: Rainstorms in China, China Water Power Press, China, 397-422, 2002.

Ye B, Li C, Yang D, et al.: Variation Trend of Precipitation and Its Impact on Water Resources in China during Last 50 Years(I): Annual Variation, Journal of Glaciology and Geocryology, 26, 588-594, 2004.

Zhu Y, Wang H, Zhou W, et al.: Recent changes in the summer precipitation pattern in East China and the background circulation, Climate Dynamics, 36, 1463-1473, 2011.

Hydrol. Earth Syst. Sci. Discuss., https://doi.org/10.5194/hess-2017-756
Manuscript under review for journal Hydrol. Earth Syst. Sci.
Discussion started: 17 January 2018

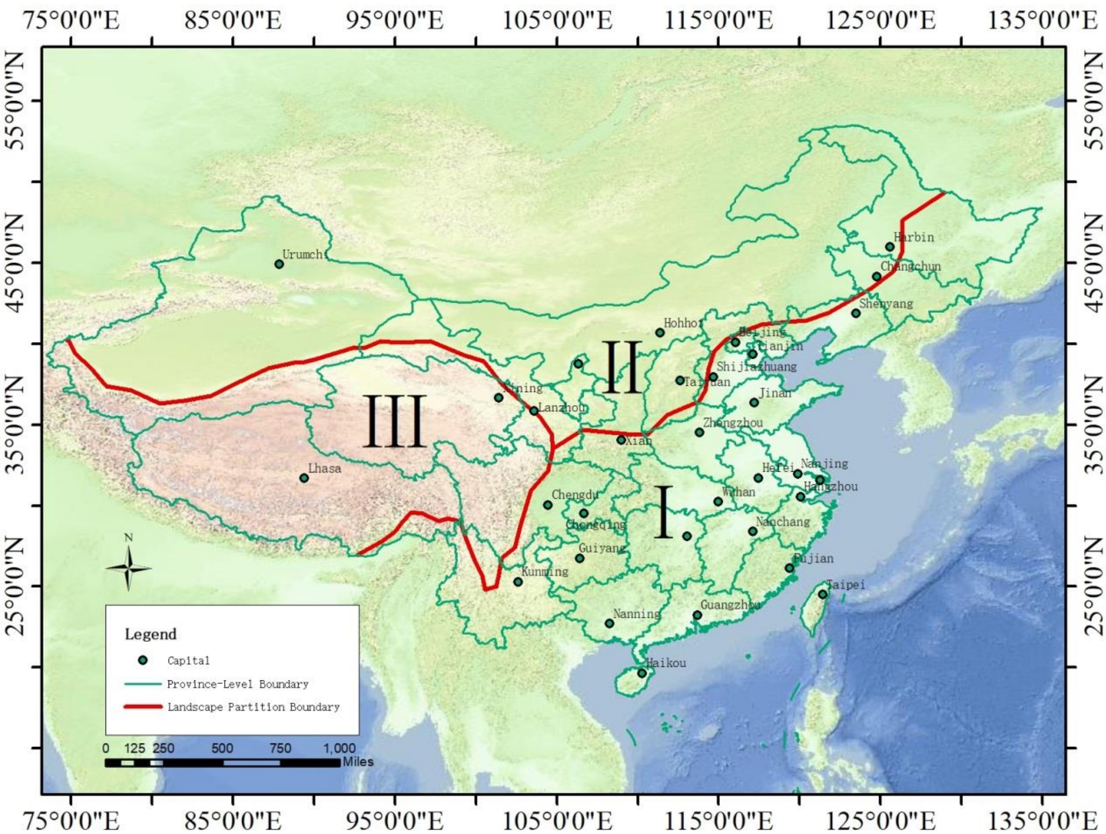

Figure 1 China Landscape Map with Storm Zoning

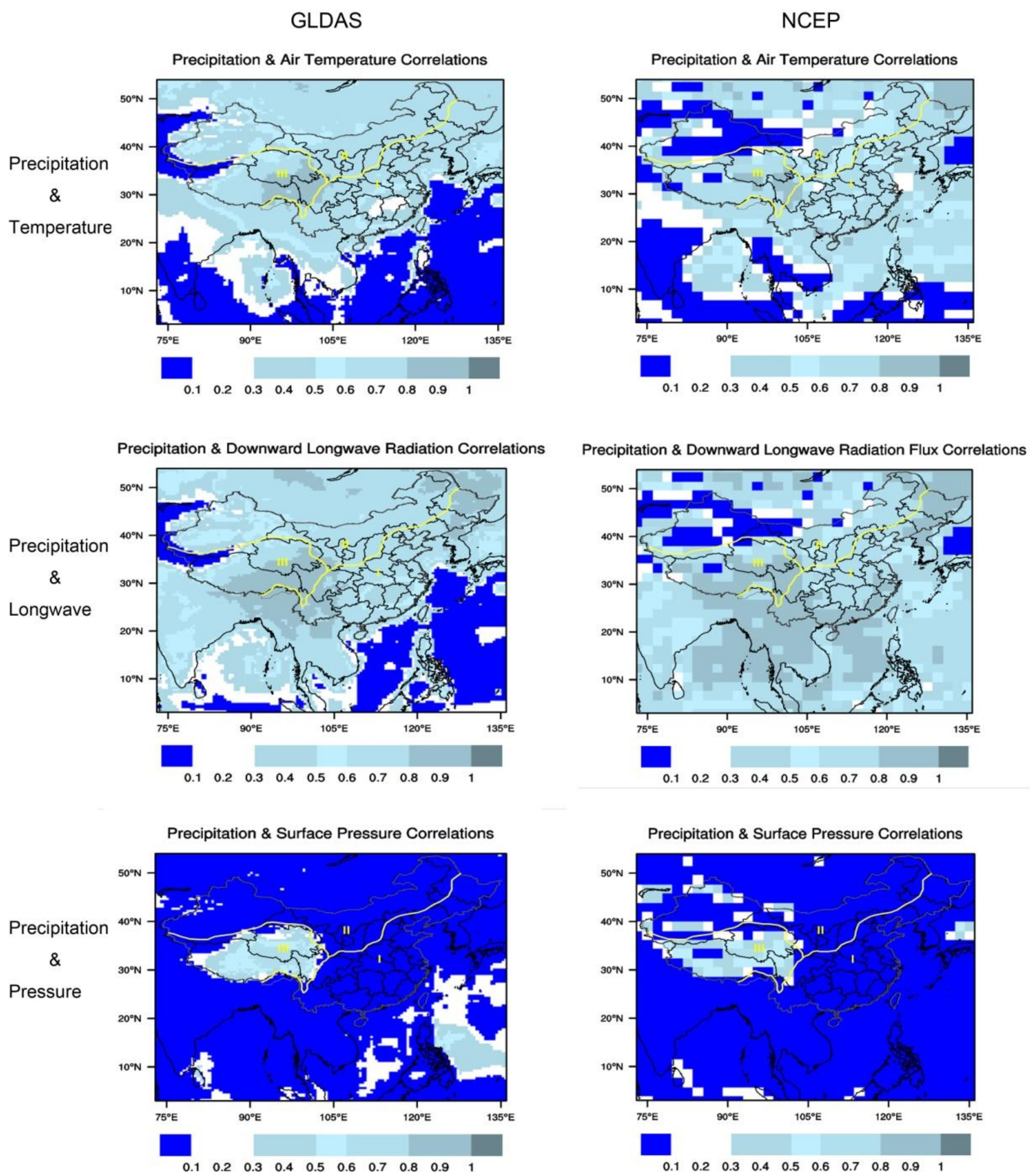

Figure 2 Correlation of precipitation and other meteorological factors (temperature/longwave/pressure) by GLDAS and NCEP (r=0.086 at a 99% confidence level)

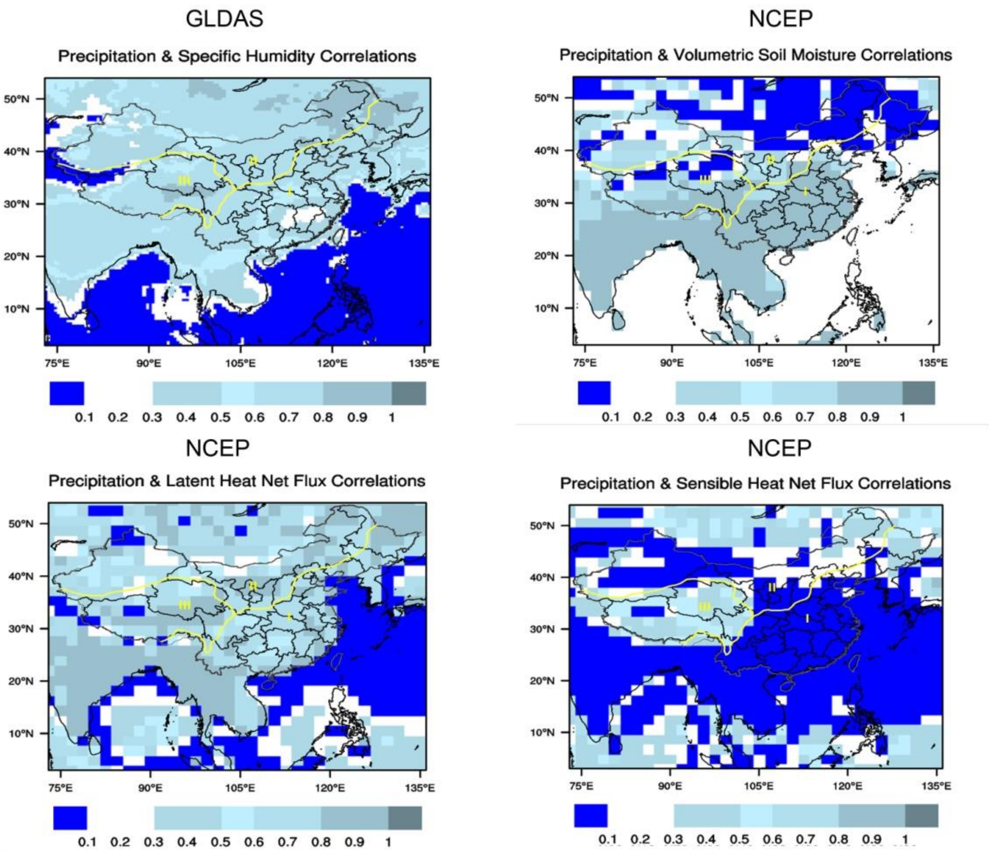

Figure 3 Correlation of precipitation and other meteorological factors (humidity/soil moisture/latent heat/sensible heat) by GLDAS and NCEP (r=0.086 at a 99% confidence level)

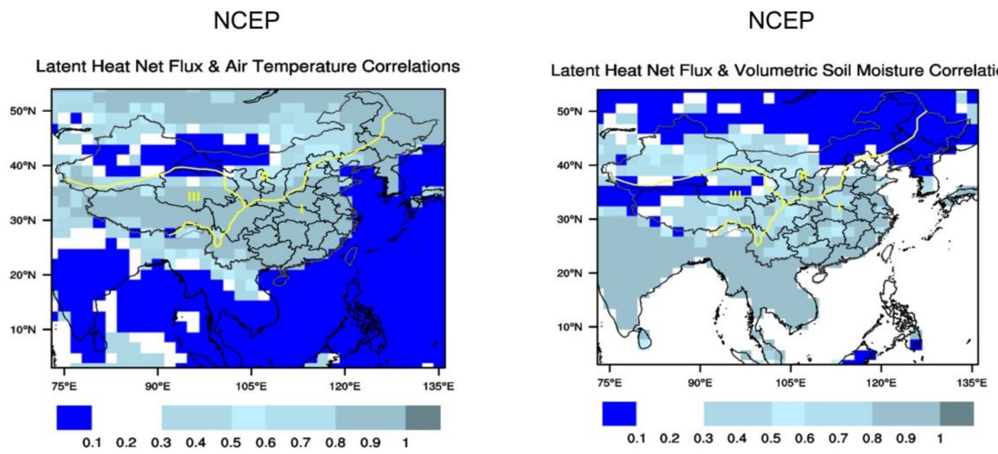

Figure 4 Correlation of latent heat and other meteorological factors (temperature/soil moisture) by NCEP (r=0.086 at 99% confidence level)

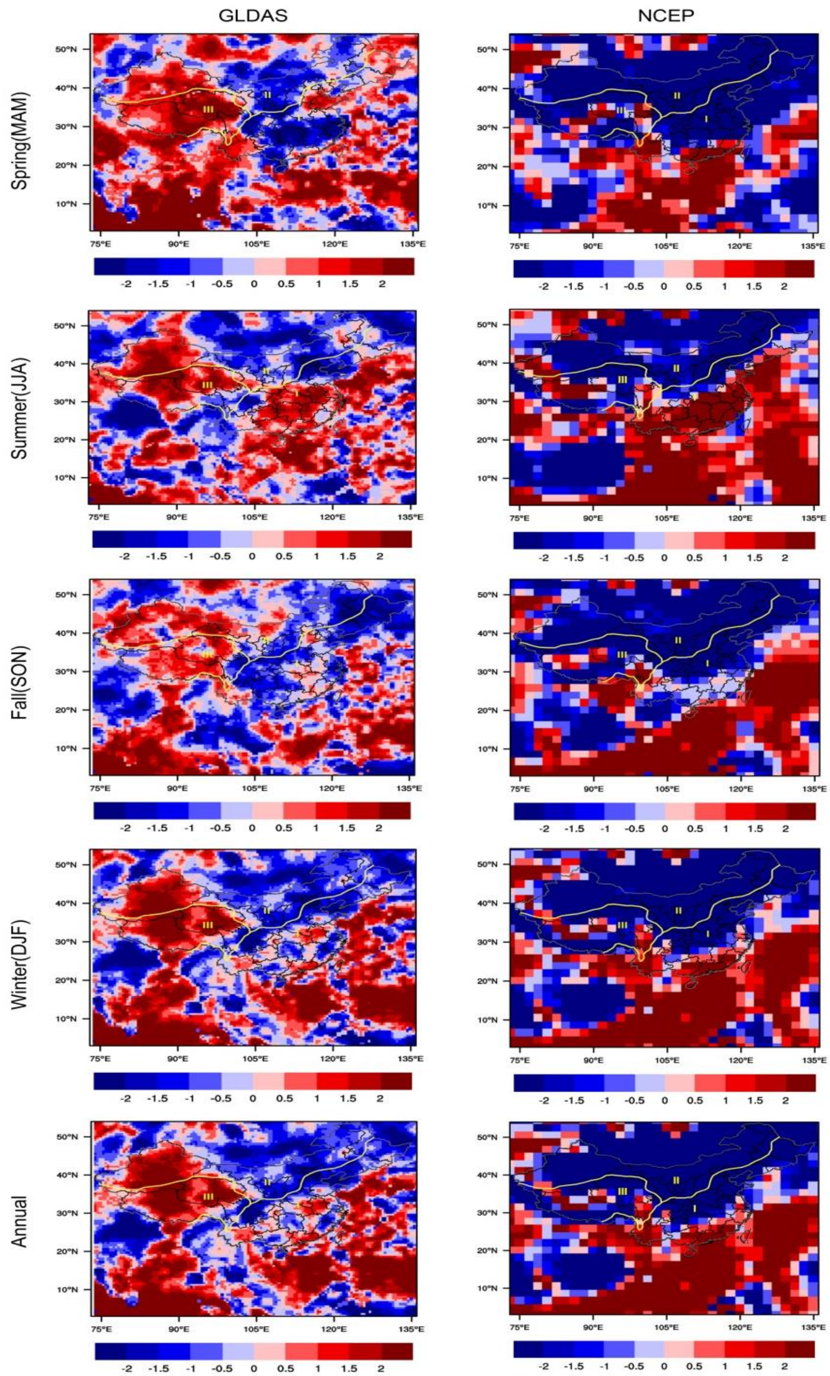

Figure 5 Mann-Kendall test Z values by GLDAS and NCEP for precipitation (Z=1.96 at 95% confidence level)

Hydrol. Earth Syst. Sci. Discuss., https://doi.org/10.5194/hess-2017-756
Manuscript under review for journal Hydrol. Earth Syst. Sci.
Discussion started: 17 January 2018

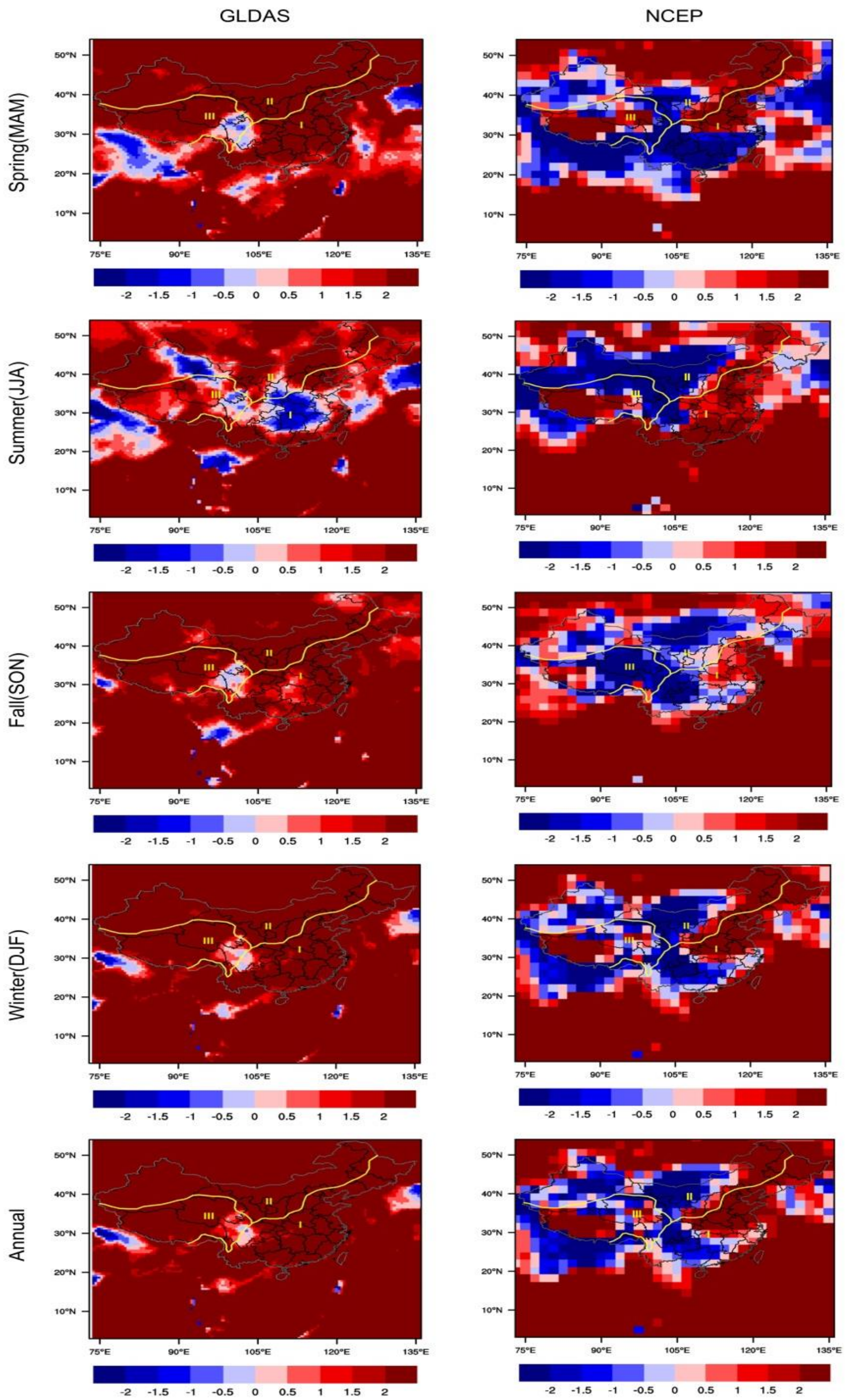

Figure 6 Mann-Kendall test Z values by GLDAS and NCEP for surface temperature (Z=1.96 at 95% confidence level)

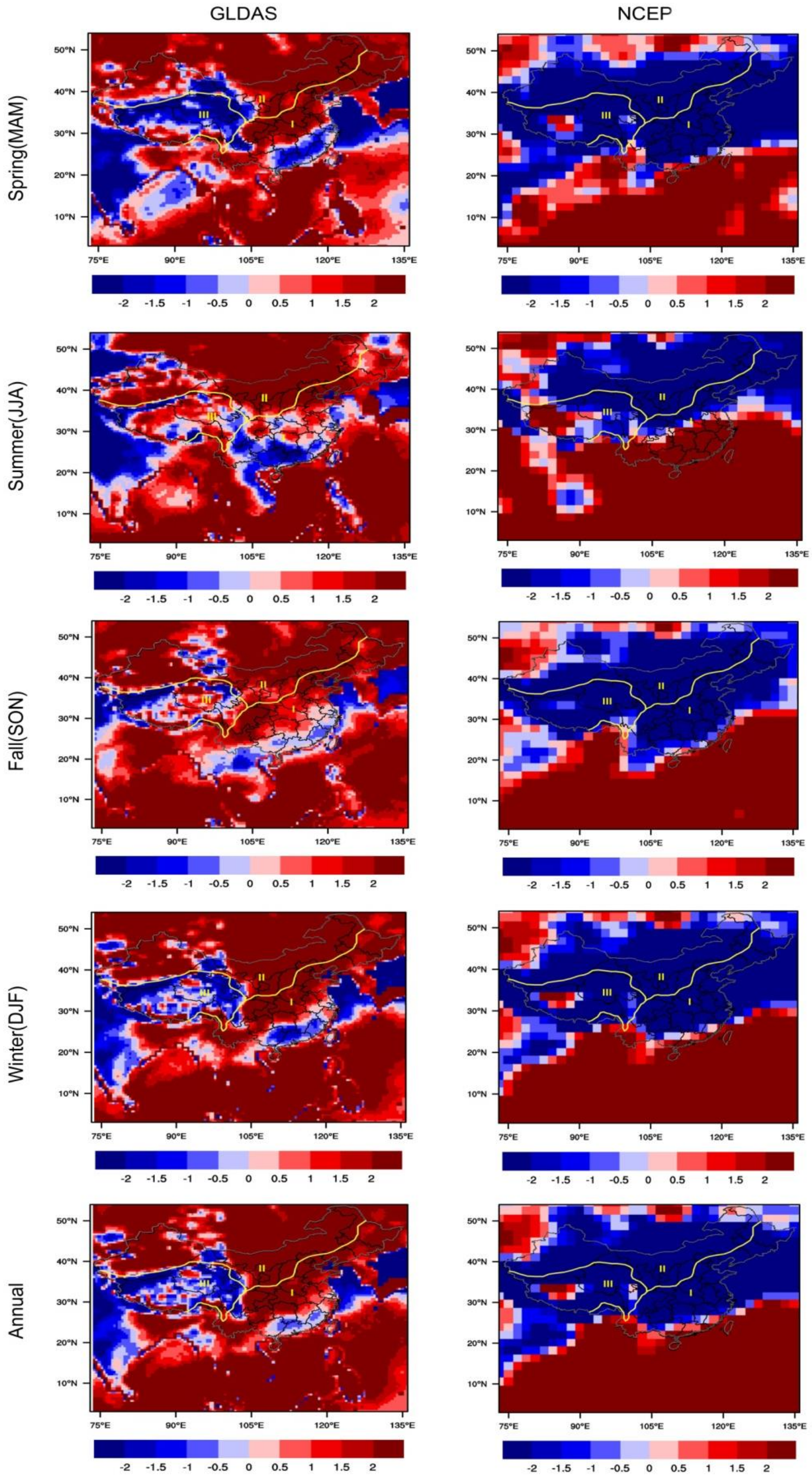
GLDAS
NCEP
Spring(MAM)
Summer(JJA)
Fall(SON)
Winter(DJF)
Annual
-2 -1.5 -1 -0.5 0 0.5 1 1.5 2

24

Hydrology and Earth System Sciences
Open Access
Discussions

Figure 7 Mann-Kendall test Z values by GLDAS and NCEP for downward longwave radiation (Z=1.96 at 95% confidence level)

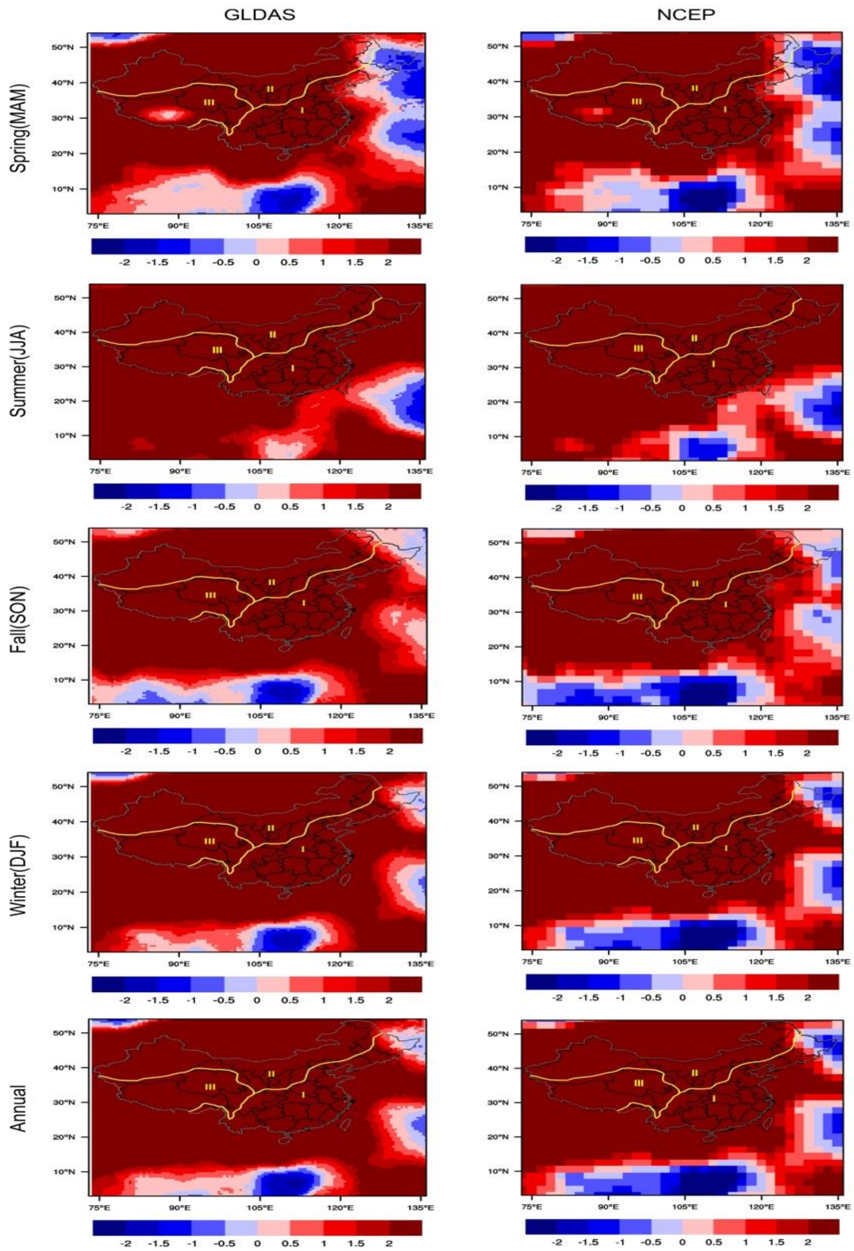

Figure 8 Mann-Kendall test Z values by GLDAS and NCEP for surface pressure (Z=1.96 at 95% confidence level)

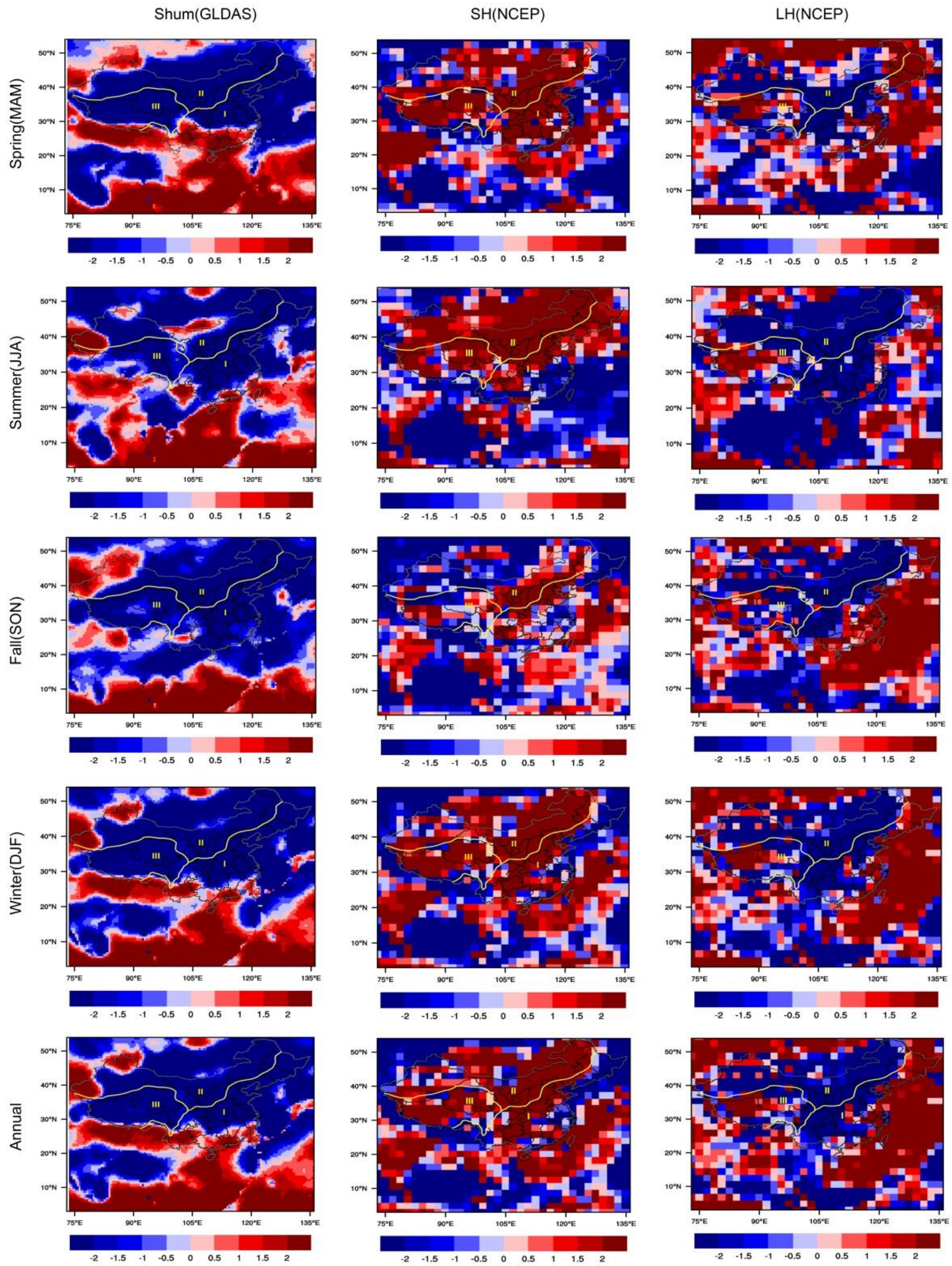

Figure 9 Mann-Kendall test Z values for humidity by GLDAS and for sensible/latent heat by NCEP (Z=1.96 at 95% confidence level)

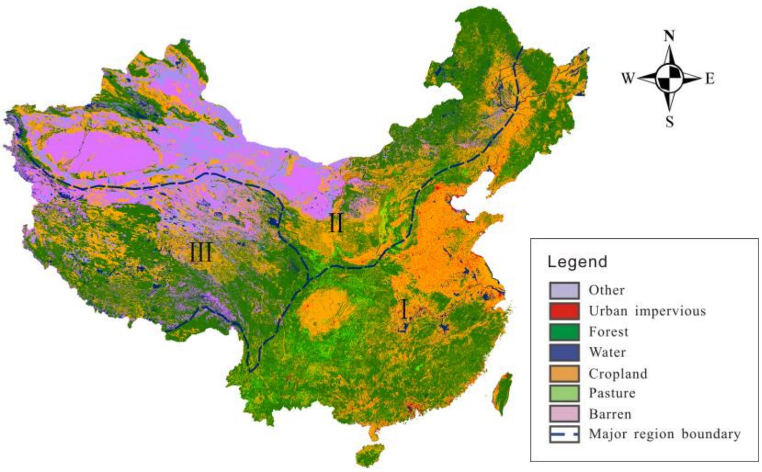

Figure 10 Land Use Map